Dynamic thermo-mechanical coupled response of random particulate composites: A statistical two-scale method*

Yang Zi-Hao(杨自豪)[a)†], Chen Yun(陈 云)[b)], Yang Zhi-Qiang(杨志强)[a)], and Ma Qiang(马 强)[c)]

[a)] *Department of Applied Mathematics, Northwestern Polytechnical University, Xi'an* 710129, *China*
[b)] *College of Computer Science, Fujian Agriculture and Forestry University, Fuzhou* 350002, *China*
[c)] *LSEC, ICMSEC, Academy of Mathematics and Systems Science, Chinese Academy of Sciences, Beijing* 100190, *China*

(Received 5 November 2013; revised manuscript received 19 February 2014; published online 28 May 2014)

This paper focuses on the dynamic thermo-mechanical coupled response of random particulate composite materials. Both the inertia term and coupling term are considered in the dynamic coupled problem. The formulation of the problem by a statistical second-order two-scale (SSOTS) analysis method and the algorithm procedure based on the finite-element difference method are presented. Numerical results of coupled cases are compared with those of uncoupled cases. It shows that the coupling effects on temperature, thermal flux, displacement, and stresses are very distinct, and the micro-characteristics of particles affect the coupling effect of the random composites. Furthermore, the coupling effect causes a lag in the variations of temperature, thermal flux, displacement, and stresses.

Keywords: random particulate composites, statistical second-order two-scale (SSOTS) analysis method, thermo-mechanical coupling effect, numerical algorithm

PACS: 65.40.–b, 68.35.–p **DOI:** 10.1088/1674-1056/23/7/076501

1. Introduction

The classical theory of coupled thermoelasticity based on Fourier's law is developed by Biot and others.[1,2] A mutual interaction exists between the displacement and temperature fields in the fully coupled problem. However, some simplifications in the conventional analysis for the coupled theory of thermoelasticity are usually made. The researchers often assume that the inertia term may be neglected in the motion equation and the thermo-mechanical coupling term may be neglected in the heat conduction equation. However, for many actual situations in science and engineering, such as thermal shock problems in nuclear reactors and structures of space craft, it is necessary to retain the fully coupled theory.[2–4] Up to now, extensive research has been performed on the thermo-mechanical problem for various structures made of single materials with different initial-boundary conditions. Various methods, including the Laplace transform and Fourier transform, finite-element (FE) method, finite difference method, and finite boundary method, have been developed and applied to solve the thermo-mechanical problems analytically or numerically.[5–9] However, the dynamic coupled thermo-mechanical problem became more complicated with the appearance of the coupling term and the work done in the field is relatively limited. Ma *et al.*[10] analyzed the fully coupled problem of a thin plate by using the precise time-integration method. Lee *et al.*[11] applied the Laplace transform and the finite difference method to solve the dynamic thermo-mechanical problem of an annular fin, and Abd-Alla *et al.*[4] considered the same problem by using an implicit finite difference algorithm. Farhat *et al.*[12] proposed an unconditionally stable staggered procedure for the finite-element solutions of the dynamic and coupled problem.

In recent years, composite materials have been widely encountered in engineering applications owing to their attractive physical and mechanical properties. In modern industries including aerospace, nuclear, and automobile, many composite structures work under the thermo-mechanical coupling environments. Thus, the study on the dynamic thermo-mechanical coupled problem for composites has practical significance in designing and optimizing the composite materials. Nevertheless, so far, most research on the thermo-mechanical problem has focused on periodic composites and/or neglected the coupling term to simplify the problem.[13–18] Francfort[19] and Parnell[20] have given the homogenized procedure for the dynamic problem of periodic composite. Aboudi[21] studied the dynamic coupled problem for multiphase composites and some valueable results have been given. However, the results of the problems for the random composites is unfortunately limited in number owing to the complexity of the structures of random composite materials.[22,23] Moreover, to our konwledge, we have not seen such results of the dynamic thermo-mechanical coupled problem for the random composites, including the investigations on the thermo-mechanical coupling effect.

*Project supported by the Special Funds for the National Basic Research Program of China (Grant No. 2012CB025904) and the National Natural Science Foundation of China (Grant Nos. 90916027 and 11302052).

†Corresponding author. E-mail: yzh@mail.nwpu.edu.cn

© 2014 Chinese Physical Society and IOP Publishing Ltd

Since the random composites have complex and varying microstructure, in order to capture the local fluctuation behaviors of temperature and displacement fields and their derivatives, the mesh size must be very small while employing traditional finite element method, which leads to tremendous amout of computer memory and CPU time. Thus, in recent years, based on the homogenization method,[24] Cui *et al.* introduced a higher-order multi-scale method to predict physical and mechanical behaviors of composites.[25–27] Based on the second-order two-scale method, Wan[28] studied the dynamic thermo-mechanical problem of periodic composite materials. After that, Cui *et al.* estabished the statistical second-order two-scale analysis method by introducing the random sample model to predict physical and mechanical properties of random materials.[29–31] Then, Yang *et al.*[32] studied the dynamic coupled thermoelastic problem of the random composites by the SSOTS method. The feasibility of the method has been validated in Ref. [32]. Based on previous research, this paper mainly focuses on the thermo-mechanical coupling effect and the influences of micro-characteristics of particles, including their shape, size, spatial distribution, and volume fraction, on the macroscopic behaviors and coupling effect. The difference between the coupling effect in microscopic scale and that in macroscopic scale is also analyzed.

This paper is organized as follows. The SSOTS formulation and related algorithm procedure based on the finite-element difference method are briefly presented in Sections 2 and 3. In Section 4, numerical results for the thermo-mechanical coupling effect are given. The paper closes with a conclusion in Section 5.

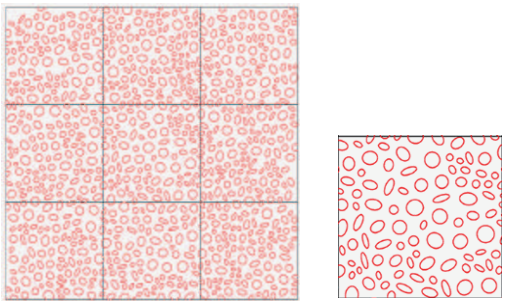
For convenience, Einstein summation convention on repeated indices is used and C denotes positive constants throughout this paper.

2. Setting of problem and SSOTS formulation

2.1. Representation of microscopic configurations of random composites

Suppose that the investigated structure Ω is made from matrix and particles. All the particles are considered as ellipsoids or polyhedrons inscribed inside ellipsoids, which are randomly distributed in the matrix.[30] In this paper, all the ellipsoid particles are considered as "one-scale", which means all of their long axes satisfy $r_1 < a < r_2$, where r_1 and r_2 give lower and upper bounds. Then the composite material with random distribution of particles can be represented as follows.

(i) There exists a constant ε ($a \ll \varepsilon \ll L$), where L is the size of Ω. Thus the structure Ω can be considered as a set of cells with ε size, as shown in Fig. 1. The probability distribution of the particles in each cell is the same as each other. Then the investigated structure has periodically random distribution of particles, and then can be represented by the probability distribution of the particles inside a typical cell.



(a) (b)

Fig. 1. (color online) (a) A part of investigated structure Ω; (b) the particle distribution of one sample.

(ii) Each random ellipsoid in three-dimensional apace is defined by nine random parameters, i.e., the coordinates of the central point (x_1, x_2, x_3), the sizes of the long, middle, and short axis (a, b, c), and three orientation parameters of the long and middle axis $(\theta_{ax_1x_2}, \theta_{ax_1}, \theta_{bx_1x_2})$. If there are I ellipsoids in a cell εY^s, Y^s represents a normalized cell, then a sample of particle distribution is defined as follows:

$$\omega^{\mathrm{s}} = (x_{11}, x_{21}, x_{31}, a_1, b_1, c_1, \theta_{ax_1x_21}, \theta_{ax_11}, \theta_{bx_1x_21}, \ldots, x_{1I}, x_{2I}, x_{3I}, a_I, b_I, c_I, \theta_{ax_1x_2I}, \theta_{ax_1I}, \theta_{bx_1x_2I}).$$

Therefore, the structure Ω is logically composed of ε-size cells subjected to the identical probability distribution model $\mathcal{P}$ and

$$\Omega = \bigcup_{s=1}^{m} {}_{(\omega^{\mathrm{s}}, z\in Z)} \varepsilon(Y^{\mathrm{s}} + z),$$

where $s = 1, 2, 3, \ldots$, denotes the index of samples and Z is the integer set. For the whole Ω, we define

$$\omega = \{\omega^{\mathrm{s}} \,|\, x \in \varepsilon Y^{\mathrm{s}} \subset \Omega\}.$$

Thus, the material parameters of the random composite materials used in the following dynamic thermo-mechanical coupled problem (1) can be periodically expressed as $A^\varepsilon(x, \omega)$, and for a sample ω^{s}, the parameters $A^\varepsilon(x, \omega^{\mathrm{s}})$ can be defined as follows:

$$A^\varepsilon(x, \omega^{\mathrm{s}}) = \begin{cases} A^1, & x \in \bigcup_{i=1}^{I} e_i, \\ A^2, & x \in \varepsilon Y^{\mathrm{s}} - \bigcup_{i=1}^{I} e_i, \end{cases}$$

where $\bigcup_{i=1}^{I} e_i$ denotes the domain of the I ellipsoids, and A^1 and A^2 are constants satisfying $\left|\max\{A^1, A^2\}\right| < C$.

In order to avoid the arguments on the mathematical properties of investigated functions below, we suppose that the random material parameters $A^\varepsilon(x, \omega^{\mathrm{s}})$ are bounded measurable functions of the random variable ω^{s}, and their mathematical expectations exist.

2.2. SSOTS formulation

Based on previous representation, the mixed initial-boundary value problem of the dynamic thermo-mechanical coupled behavior can be expressed as follows:

$$\begin{cases} \rho^{\varepsilon}(x,\omega)c^{\varepsilon}(x,\omega)\dfrac{\partial T^{\varepsilon}(x,\omega,t)}{\partial t} \\ +\tilde{T}\beta_{ij}^{\varepsilon}(x,\omega)\dfrac{\partial}{\partial t}\left(\dfrac{\partial u_i^{\varepsilon}(x,\omega,t)}{\partial x_j}\right) \\ -\dfrac{\partial}{\partial x_i}\left(k_{ij}^{\varepsilon}(x,\omega)\dfrac{\partial T^{\varepsilon}(x,\omega,t)}{\partial x_j}\right)=h, \quad \text{in } \Omega\times(0,\breve{t}), \\ \rho^{\varepsilon}(x,\omega)\dfrac{\partial^2 u_i^{\varepsilon}(x,\omega,t)}{\partial t^2}-\dfrac{\partial}{\partial x_j}\Bigg(C_{ijkl}^{\varepsilon}(x,\omega)\dfrac{\partial u_k^{\varepsilon}(x,\omega,t)}{\partial x_l} \\ -\beta_{ij}^{\varepsilon}(x,\omega)\left(T^{\varepsilon}(x,\omega,t)-\tilde{T}\right)\Bigg)=f_i, \quad \text{in } \Omega\times(0,\breve{t}) \\ T^{\varepsilon}(x,\omega,t)=\hat{T}, \quad \text{on } \Gamma_T\times(0,\breve{t}), \\ \boldsymbol{u}^{\varepsilon}(x,\omega,t)=\hat{\boldsymbol{u}}, \quad \text{on } \Gamma_u\times(0,\breve{t}), \\ n_i k_{ij}^{\varepsilon}(x,\omega)\dfrac{\partial T^{\varepsilon}}{\partial x_j}=\bar{q}, \quad \text{on } \Gamma_q\times(0,\breve{t}), \\ n_j\Bigg(C_{ijkl}^{\varepsilon}(x,\omega)\dfrac{\partial u_k^{\varepsilon}(x,\omega,t)}{\partial x_l} \\ -\beta_{ij}^{\varepsilon}(x,\omega)\left(T^{\varepsilon}(x,\omega,t)-\tilde{T}\right)\Bigg)=\bar{\sigma}_i, \quad \text{on } \Gamma_t\times(0,\breve{t}), \\ T^{\varepsilon}(x,\omega,0)=\tilde{T}, \quad \boldsymbol{u}^{\varepsilon}(x,\omega,0)=\tilde{\boldsymbol{u}}, \\ \dfrac{\partial \boldsymbol{u}^{\varepsilon}}{\partial t}(x,\omega,0)=\breve{\boldsymbol{u}}, \quad \text{in } \Omega, \\ (\Gamma_T\cap\Gamma_q=\emptyset,\ \Gamma_u\cap\Gamma_t=\emptyset,\ \Gamma_T\cup\Gamma_q=\Gamma_t\cup\Gamma_u=\partial\Omega), \end{cases} \tag{1}$$

where $i,j,k,l=1,2,3$; $T^{\varepsilon}(x,t)$ and $\boldsymbol{u}^{\varepsilon}(x,t)$ denote the temperature and displacement; $\rho^{\varepsilon}(x,\omega)$ and $c^{\varepsilon}(x,\omega)$ are the mass density and specific heat; $\beta_{ij}^{\varepsilon}(x,\omega)$, $C_{ijkl}^{\varepsilon}(x,\omega)$, and $k_{ij}^{\varepsilon}(x,\omega)$ are the thermal modulus, elastic tensor, and thermal conductivity, respectively; $h(x,t)$ and $f_i(x,t)$ are the internal heat source and the body force; $\hat{T}$ is the prescribed temperature on the boundary Γ_T, $\hat{\boldsymbol{u}}$ is the prescribed displacements on the boundary Γ_u; $\bar{q}$ is the heat flux prescribed normal to the boundary Γ_q; $\bar{\sigma}_i$ is the prescribed tractions on the boundary Γ_t, n_i and n_j are the normal direction cosine of Γ_q and Γ_t, respectively; $\tilde{T}$, $\tilde{\boldsymbol{u}}$, and $\breve{\boldsymbol{u}}$ are the initial temperature, displacement, and velocity field, respectively.

Let $y=x/\varepsilon\in Y$ denotes the local coordinates on the normalized cell Y. Then the material parameters in Y can be expressed as $A^{\varepsilon}(x,\omega)=A(y,\omega)$. Since $T^{\varepsilon}(x,\omega,t)$ and $\boldsymbol{u}^{\varepsilon}(x,\omega,t)$ of problem (1) depend on both the global behaviors and random microscopic configurations, they can be expressed as $T^{\varepsilon}(x,\omega,t)=T(x,y,\omega,t)$ and $\boldsymbol{u}^{\varepsilon}(x,\omega,t)=\boldsymbol{u}(x,y,\omega,t)$.

Since the investigated structure is periodically random, inspired by Refs. [32] and [28] and in the constructive way, it is assumed that $T^{\varepsilon}(x,\omega,t)$ and $\boldsymbol{u}^{\varepsilon}(x,\omega,t)$ can be expanded into the series of the following forms in two-scale variables x, y:

$$\begin{aligned} & T^{\varepsilon}(x,\omega,t) \\ &= T_0(x,t)+\varepsilon M_{\alpha_1}(y,\omega)\frac{\partial T_0(x,t)}{\partial x_{\alpha_1}} \\ &\quad +\varepsilon^2\left(M_{\alpha_1\alpha_2}(y,\omega)\frac{\partial^2 T_0(x,t)}{\partial x_{\alpha_1}\partial x_{\alpha_2}}+R_{\alpha_1\alpha_2}(y,\omega)\frac{\partial^2 u_{0\alpha_1}(x,t)}{\partial t\partial x_{\alpha_2}}\right. \\ &\quad \left.+Q_2(y,\omega)\frac{\partial T_0(x,t)}{\partial t}\right)+\varepsilon^3 Z_1(x,y,\omega), \end{aligned} \tag{2}$$

$$\begin{aligned} & \boldsymbol{u}^{\varepsilon}(x,\omega,t) \\ &= \boldsymbol{u}_0(x,t)+\varepsilon\left(\boldsymbol{N}_{\alpha_1}(y,\omega)\frac{\partial \boldsymbol{u}_0(x,t)}{\partial x_{\alpha_1}}\right. \\ &\quad \left.-\boldsymbol{P}_0(y,\omega)\left(T_0(x,t)-\tilde{T}\right)\right) \\ &\quad +\varepsilon^2\left(\boldsymbol{N}_{\alpha_1\alpha_2}(y,\omega)\frac{\partial^2 \boldsymbol{u}_0(x,t)}{\partial x_{\alpha_1}\partial x_{\alpha_2}}-\boldsymbol{P}_{\alpha_1}(y,\omega)\frac{\partial T_0(x,t)}{\partial x_{\alpha_1}}\right. \\ &\quad \left.-\boldsymbol{F}_2(y,\omega)\frac{\partial^2 \boldsymbol{u}_0(x,t)}{\partial t^2}\right)+\varepsilon^3\boldsymbol{Z}_2(x,y,\omega), \end{aligned} \tag{3}$$

where $T_0(x,t)$ and $\boldsymbol{u}_0(x,t)$ only reflect the macroscopic behaviors, and are called the homogenized solutions; $\boldsymbol{N}_{\alpha_1}(y,\omega)$, $\boldsymbol{N}_{\alpha_1\alpha_2}(y,\omega)$, and $\boldsymbol{F}_2(y,\omega)$ are matrix-valued functions; $\boldsymbol{P}_0(y,\omega)$ and $\boldsymbol{P}_{\alpha_1}(y,\omega)$ are vector-valued functions defined on the unit cell Y, which involve the microstructural information. They will be determined below.

Due to $y=x/\varepsilon\in Y$, respecting the chain rule as $\partial/\partial x_i\to\partial/\partial x_i+(1/\varepsilon)\times(\partial/\partial y_i)$, we substitute Eqs. (2) and (3) into Eq. (1) and the match terms of the same order of ε, then a series of equations are obtained if the coefficients of $\varepsilon^l(l=-1,0,1,\ldots,)$ from both sides are required to equal each other.

From the coefficients of ε^{-1}, for any sample ω^{s}, the following local cell problems defined on Y^{s} for $M_{\alpha_1}(y,\omega)$, $\boldsymbol{N}_{\alpha_1}(y,\omega)$, and $\boldsymbol{P}_0(y,\omega)$ are constructed:

$$\begin{cases} -\dfrac{\partial}{\partial y_i}\left(k_{ij}(y,\omega^{\mathrm{s}})\dfrac{\partial M_{\alpha_1}(y,\omega^{\mathrm{s}})}{\partial y_j}\right) \\ =\dfrac{\partial}{\partial y_i}\left(k_{i\alpha_1}(y,\omega^{\mathrm{s}})\right), \quad y\in Y^{\mathrm{s}}, \\ M_{\alpha_1}(y,\omega^{\mathrm{s}})=0, \quad y\in\partial Y^{\mathrm{s}}, \end{cases} \tag{4}$$

$$\begin{cases} -\dfrac{\partial}{\partial y_j}\left(C_{ijkl}(y,\omega^{\mathrm{s}})\dfrac{\partial \boldsymbol{N}_{\alpha_1 km}(y,\omega^{\mathrm{s}})}{\partial y_l}\right) \\ =\dfrac{\partial}{\partial y_j}\left(C_{ijm\alpha_1}(y,\omega^{\mathrm{s}})\right), \quad y\in Y^{\mathrm{s}}, \\ \boldsymbol{N}_{\alpha_1 m}(y,\omega^{\mathrm{s}})=0, \quad y\in\partial Y^{\mathrm{s}}, \end{cases} \tag{5}$$

$$\begin{cases} -\dfrac{\partial}{\partial y_j}\left(C_{ijkl}(y,\omega^{\mathrm{s}})\dfrac{\partial \boldsymbol{P}_{0k}(y,\omega^{\mathrm{s}})}{\partial y_l}\right) \\ =\dfrac{\partial}{\partial y_j}\left(\beta_{ij}(y,\omega^{\mathrm{s}})\right), \quad y\in Y^{\mathrm{s}}, \\ \boldsymbol{P}_0(y,\omega^{\mathrm{s}})=0, \quad y\in\partial Y^{\mathrm{s}}. \end{cases} \tag{6}$$

Inspired by Ref. [28] and from $M_{\alpha_1}(y,\omega)$, $\boldsymbol{N}_{\alpha_1}(y,\omega)$, and $\boldsymbol{P}_0(y,\omega)$, for any sample ω^{s} the homogenization specific heat capacity $\hat{S}(\omega^{\mathrm{s}})$, thermal conductivity $\hat{k}_{ij}(\omega^{\mathrm{s}})$, thermal modulus $\hat{\beta}_{ij}(\omega^{\mathrm{s}})$, mass density $\hat{\rho}(\omega^{\mathrm{s}})$, and elasticity tensor $\hat{C}_{ijkl}(\omega^{\mathrm{s}})$ are defined as

$$\hat{S}(\omega^{\mathrm{s}}) = \frac{1}{|Y^{\mathrm{s}}|}\int_{Y^{\mathrm{s}}}\Big(\rho(y,\omega^{\mathrm{s}})c(y,\omega^{\mathrm{s}})$$

$$
\begin{aligned}
&-\tilde{T}\beta_{ij}(y,\omega^{\mathrm{s}})\frac{\partial \boldsymbol{P}_{0i}(y,\omega^{\mathrm{s}})}{\partial y_j}\Big)\,\mathrm{d}y,\\
\hat{k}_{ij}(\omega^{\mathrm{s}}) &= \frac{1}{|Y^{\mathrm{s}}|}\int_{Y^{\mathrm{s}}}\left(k_{ij}(y,\omega^{\mathrm{s}})+k_{ik}(y,\omega^{\mathrm{s}})\frac{\partial M_j(y,\omega^{\mathrm{s}})}{\partial y_k}\right)\mathrm{d}y,\\
\hat{\beta}_{ij}(\omega^{\mathrm{s}}) &= \frac{1}{|Y^{\mathrm{s}}|}\int_{Y^{\mathrm{s}}}\Big(\beta_{ij}(y,\omega^{\mathrm{s}})\\
&\quad+\beta_{kl}(y,\omega^{\mathrm{s}})\frac{\partial \boldsymbol{N}_{jki}(y,\omega^{\mathrm{s}})}{\partial y_l}\Big)\,\mathrm{d}y,\\
\hat{\rho}(\omega^{\mathrm{s}}) &= \frac{1}{|Y^{\mathrm{s}}|}\int_{Y^{\mathrm{s}}}\rho(y,\omega^{\mathrm{s}})\,\mathrm{d}y,\\
\hat{C}_{ijkl}(\omega^{\mathrm{s}}) &= \frac{1}{|Y^{\mathrm{s}}|}\int_{Y^{\mathrm{s}}}\Big(C_{ijkl}(y,\omega^{\mathrm{s}})\\
&\quad+C_{ijm\alpha_1}(y,\omega^{\mathrm{s}})\frac{\partial \boldsymbol{N}_{lmk}(y,\omega^{\mathrm{s}})}{\partial y_{\alpha_1}}\Big)\,\mathrm{d}y. \qquad (7)
\end{aligned}
$$

From the above suppositions, Theorem 2.1 in Ref. [29] and Lemma 3.2 in Ref. [30], it follows that $\hat{k}_{ij}(\omega^{\mathrm{s}})$ and $\hat{C}_{ijkl}(\omega^{\mathrm{s}})$ are bounded functions with respect to the random variable. Similarly, it is easy to prove that $\hat{S}(\omega^{\mathrm{s}})\hat{\beta}_{ij}(\omega^{\mathrm{s}})$ and $\hat{\rho}(\omega^{\mathrm{s}})$ are also bounded. Then from the suppositions, the mathematical expectations of those functions exist. Therefore, by taking r samples $(\omega^{\mathrm{s}}, s=1,2,\ldots,r)$ and from Kolmogorov's classical strong law of large numbers, the expected homogenized parameters can be calculated by

$$
\begin{aligned}
&\widehat{S}=\lim_{r\to\infty}\frac{\sum_{s=1}^{r}\hat{S}(\omega^{\mathrm{s}})}{r},\quad \widehat{k}_{ij}=\lim_{r\to\infty}\frac{\sum_{s=1}^{r}\hat{k}_{ij}(\omega^{\mathrm{s}})}{r},\\
&\widehat{\beta}_{ij}=\lim_{r\to\infty}\frac{\sum_{s=1}^{r}\hat{\beta}_{ij}(\omega^{\mathrm{s}})}{r},\quad \widehat{\rho}=\lim_{r\to\infty}\frac{\sum_{s=1}^{r}\hat{\rho}(\omega^{\mathrm{s}})}{r},\\
&\widehat{C}_{ijkl}=\lim_{r\to\infty}\frac{\sum_{s=1}^{r}\hat{C}_{ijkl}(\omega^{\mathrm{s}})}{r}. \qquad (8)
\end{aligned}
$$

Then, we can define the homogenized equations associated with problem (1) as follows:

$$
\begin{cases}
\widehat{S}\dfrac{\partial T_0(x,t)}{\partial t}+\tilde{T}\widehat{\beta}_{ij}\dfrac{\partial^2 u_{0i}(x,t)}{\partial t\partial x_j}\\
-\dfrac{\partial}{\partial x_i}\left(\widehat{k}_{ij}\dfrac{\partial T_0(x,t)}{\partial x_j}\right)=h,\quad \text{in } \Omega\times(0,\breve{t}),\\
\widehat{\rho}\dfrac{\partial^2 u_{0i}(x,t)}{\partial t^2}-\dfrac{\partial}{\partial x_j}\Big(\widehat{C}_{ijkl}\dfrac{\partial u_{0k}(x,t)}{\partial x_l}\\
-\widehat{\beta}_{ij}\left(T_0(x,t)-\tilde{T}\right)\Big)=f_i,\quad \text{in } \Omega\times(0,\breve{t}),\\
T_0(x,t)=\hat{T},\quad \text{on } \Gamma_T\times(0,\breve{t}),\\
\boldsymbol{u}_0(x,t)=\hat{\boldsymbol{u}},\quad \text{on } \Gamma_u\times(0,\breve{t}),\\
n_i\widehat{k}_{ij}\dfrac{\partial T_0(x,t)}{\partial x_j}=\bar{q},\quad \text{on } \Gamma_q\times(0,\breve{t}),\\
n_i\left(\widehat{C}_{ijkl}\dfrac{\partial u_{0k}}{\partial x_l}-\widehat{\beta}_{ij}\left(T_0-\tilde{T}\right)\right)=\bar{\sigma}_j,\quad \text{on } \Gamma_t\times(0,\breve{t}),\\
T_0(x,0)=\tilde{T},\quad \boldsymbol{u}_0(x,0)=\tilde{u},\\
\dfrac{\partial \boldsymbol{u}_0}{\partial t}(x,0)=\breve{\boldsymbol{u}},\quad \text{in } \Omega.
\end{cases} \qquad (9)
$$

From the coefficients of ε^0, for any sample ω^{s}, the following local cell problems defined on Y^{s} for $M_{\alpha_1\alpha_2}(y,\omega)$, $R_{\alpha_1\alpha_2}(y,\omega)$, $Q_2(y,\omega)$, $\boldsymbol{N}_{\alpha_1\alpha_2}(y,\omega)$, $\boldsymbol{F}_2(y,\omega)$, and $\boldsymbol{P}_{\alpha_1}(y,\omega)$ are constructed:

$$
\begin{cases}
-\dfrac{\partial}{\partial y_i}\left(k_{ij}(y,\omega^s)\dfrac{\partial M_{\alpha_1\alpha_2}(y,\omega^s)}{\partial y_j}\right)\\
=\dfrac{\partial}{\partial y_i}\left(k_{i\alpha_2}(y,\omega^s)M_{\alpha_1}(y,\omega^s)\right)\\
+k_{\alpha_2 j}(y,\omega^s)\dfrac{\partial M_{\alpha_1}(y,\omega^s)}{\partial y_j}\\
+k_{\alpha_1\alpha_2}(y,\omega^s)-\widehat{k}_{\alpha_1\alpha_2},\quad y\in Y^s,\\
M_{\alpha_1\alpha_2}(y,\omega^s)=0,\quad y\in\partial Y^s,
\end{cases} \qquad (10)
$$

$$
\begin{cases}
-\dfrac{\partial}{\partial y_i}\left(k_{ij}(y,\omega^s)\dfrac{\partial R_{\alpha_1\alpha_2}(y,\omega^s)}{\partial y_j}\right)\\
=\tilde{T}\Big(\widehat{\beta}_{\alpha_1\alpha_2}-\beta_{\alpha_1\alpha_2}(y,\omega^s)\\
-\beta_{ij}(y,\omega^s)\dfrac{\partial \mathrm{N}_{\alpha_2 i\alpha_1}(y,\omega^s)}{\partial y_j}\Big),\quad y\in Y^s,\\
R_{\alpha_1\alpha_2}(y,\omega^s)=0,\quad y\in\partial Y^s,
\end{cases} \qquad (11)
$$

$$
\begin{cases}
-\dfrac{\partial}{\partial y_i}\left(k_{ij}(y,\omega^s)\dfrac{\partial Q_2(y,\omega^s)}{\partial y_j}\right)\\
=\tilde{T}\beta_{ij}(y,\omega^s)\dfrac{\partial \mathrm{P}_{0i}(y,\omega^s)}{\partial y_j}\\
-\rho(y,\omega^s)c(y,\omega^s)+\widehat{S},\quad y\in Y^s,\\
Q_2(y,\omega^s)=0,\quad y\in\partial Y^s,
\end{cases} \qquad (12)
$$

$$
\begin{cases}
-\dfrac{\partial}{\partial y_j}\left(C_{ijkl}(y,\omega^s)\dfrac{\partial \mathrm{N}_{\alpha_1\alpha_2 km}(y,\omega^s)}{\partial y_l}\right)\\
=\dfrac{\partial}{\partial y_j}\left(C_{ijk\alpha_2}(y,\omega^s)\mathrm{N}_{\alpha_1 km}(y,\omega^s)\right)\\
+C_{i\alpha_1 kj}(y,\omega^s)\dfrac{\partial \mathrm{N}_{\alpha_2 km}(y,\omega^s)}{\partial y_j}\\
+C_{i\alpha_1 m\alpha_2}(y,\omega^s)-\widehat{C}_{i\alpha_1 m\alpha_2},\quad y\in Y^s,\\
\mathrm{N}_{\alpha_1\alpha_2 m}(y,\omega^s)=0,\quad y\in\partial Y^s,
\end{cases} \qquad (13)
$$

$$
\begin{cases}
\dfrac{\partial}{\partial y_j}\left(C_{ijkl}(y,\omega^s)\dfrac{\partial \mathrm{F}_{2km}(y,\omega^s)}{\partial y_l}\right)\\
=\delta_{mi}\left(\widehat{\rho}-\rho(y,\omega^s)\right),\quad y\in Y^s,\\
\boldsymbol{F}_{2m}(y,\omega^s)=0,\quad y\in\partial Y^s,
\end{cases} \qquad (14)
$$

$$
\begin{cases}
-\dfrac{\partial}{\partial y_j}\left(C_{ijkl}(y,\omega^s)\dfrac{\partial \mathrm{P}_{\alpha_1 k}(y,\omega^s)}{\partial y_l}\right)\\
=\dfrac{\partial}{\partial y_j}\left(\beta_{ij}(y,\omega^s)M_{\alpha_1}(y,\omega^s)\right)\\
+\dfrac{\partial}{\partial y_l}\left(C_{ilk\alpha_1}(y,\omega^s)\mathrm{P}_{0k}(y,\omega^s)\right)\\
+C_{i\alpha_1 kl}(y,\omega^s)\dfrac{\partial \mathrm{P}_{0k}(y,\omega^s)}{\partial y_l}+\beta_{i\alpha_1}(y,\omega^s)-\widehat{\beta}_{i\alpha_1},\quad y\in Y^s,\\
\boldsymbol{P}_{\alpha_1 k}(y,\omega^s)=0,\quad y\in\partial Y^s.
\end{cases} \qquad (15)
$$

Remark 2.1 Since the distribution of particles in all cells is random, the particle distributions in two adjacent cells are different. Therefore, the configuration of the cells cannot be

extended periodically, and the periodicity conditions cannot be used here to construct cell problems (4)–(6) and (10)–(15). In order to ensure the existence, uniqueness and the whole continuity of the solution, the zero-boundary conditions are imposed on the cell problems (4)–(6) and (10)–(15). Moreover, in problem (14), the notation δ_{mi} is the Kronecker delta function.

In practical computation of engineering, only the sum of fore three terms in Eqs. (2) and (3) are evaluated. From Eqs. (2) and (3), the SSOTS formulas of thermal flux densities and strain tensor are obtained as

$$q_i^{\varepsilon}(x,\omega,t) = -k_{ij}(y,\omega)\frac{\partial T^{\varepsilon}(x,\omega,t)}{\partial x_j}, \tag{16}$$

$$\varepsilon_{hk}^{\varepsilon}(x,\omega,t) = \frac{1}{2}\left(\frac{\partial u_h^{\varepsilon}(x,\omega,t)}{\partial x_k} + \frac{\partial u_k^{\varepsilon}(x,\omega,t)}{\partial x_h}\right). \tag{17}$$

Then the stress tensor is obtained according to Hooke's law as

$$\begin{aligned}\sigma_{ij}^{\varepsilon}(x,\omega,t) &= C_{ijhk}(y,\omega)\varepsilon_{hk}^{\varepsilon}(x,\omega,t) - \beta_{ij}(y,\omega)\\ &\quad\times\left(T^{\varepsilon}(x,\omega,t)-\tilde{T}\right).\end{aligned} \tag{18}$$

Remark 2.2 In the problem (1), the coupling term, i.e., the effect of temperature strain is considered. Equations (2) and (3) can be regarded as coupled solutions. In order to study the importance of the coupling term and its influence on the temperatures, displacements, heat flux densities and stresses, the uncoupled SSOTS formulation can be obtained in the same way. In the uncoupled case, the homogenized thermal moduli becomes

$$\hat{S}(\omega^{\mathrm{s}}) = \frac{1}{|Y^{\mathrm{s}}|}\int_{Y^{\mathrm{s}}}\rho(y,\omega^{\mathrm{s}})c(y,\omega^{\mathrm{s}})\,\mathrm{d}y. \tag{19}$$

According to the Kolmogorov's classical strong law of large numbers, the expected homogenized thermal moduli can be obtained. The first equation of homogenized problem (9) changes into Eq. (15) with a new expected homogenized thermal moduli

$$\widehat{S}(x)\frac{\partial T_0(x,t)}{\partial t} - \frac{\partial}{\partial x_i}\left(\widehat{k}_{ij}(x)\frac{\partial T_0(x,t)}{\partial x_j}\right) = h. \tag{20}$$

Based on the formal deriving process of the SSOTS method, the cell problem (12) becomes

$$\begin{cases} -\dfrac{\partial}{\partial y_i}\left(k_{ij}(y,\omega^{\mathrm{s}})\dfrac{\partial Q_2(y,\omega^{\mathrm{s}})}{\partial y_j}\right)\\ \quad = -\rho(y,\omega^{\mathrm{s}})c(y,\omega^{\mathrm{s}}) + \widehat{S}(x), \quad y\in Y^{\mathrm{s}},\\ Q_2(y,\omega^{\mathrm{s}}) = 0, \quad y\in\partial Y^{\mathrm{s}}. \end{cases} \tag{21}$$

The uncoupled solution of temperatures is obtained as

$$\begin{aligned} &T^{\varepsilon}(x,\omega,t)\\ &\cong T_0(x,t) + \varepsilon M_{\alpha_1}(y,\omega)\frac{\partial T_0(x,t)}{\partial x_{\alpha_1}}\\ &\quad+\varepsilon^2\left(M_{\alpha_1\alpha_2}(x,\omega)\frac{\partial^2 T_0(x,t)}{\partial x_{\alpha_1}\partial x_{\alpha_2}} + Q_2(x,\omega)\frac{\partial T_0(x,t)}{\partial t}\right). \end{aligned} \tag{22}$$

3. Finite-element difference implementation of the SSOTS method

The computer simulation algorithm developed in Ref. [33] is used to generate a sample with random particles, and the FE meshes applied in this study are those of Ref. [34]. The homogenization problem (9) is dynamic and strongly coupled by hyperbolic and parabolic equations. Hence, the spatial region Ω is divided by using the FE meshes first, then the temporal domain $(0,\breve{t})$ is divided by using the finite difference. The heat equation is integrated over time using the backward difference scheme,[35] and the Newmark difference scheme[35] is used for the dynamical equation. Now the algorithm procedure for predicting the dynamic thermo-mechanical coupled response by the SSOTS method is presented as follows.

(i) Generate a sample cell according to the random probability distribution model $\mathcal{P}$ and determine the material parameters mentioned in problem (1). Then generate its FE meshes.

(ii) Solve problems (4)–(6) to obtain $M_{\alpha_1}(y,\omega^{\mathrm{s}})$, $\boldsymbol{N}_{\alpha_1}(y,\omega^{\mathrm{s}})$, and $\boldsymbol{P}_0(y,\omega^{\mathrm{s}})$ by the finite-element method, and then calculate the homogenized parameters $\hat{S}(\omega^{\mathrm{s}})$, $\hat{k}_{ij}(\omega^{\mathrm{s}})$, $\hat{\beta}_{ij}(\omega^{\mathrm{s}})$, $\hat{\rho}(\omega^{\mathrm{s}})$, and $\hat{C}_{ijkl}(\omega^{\mathrm{s}})$ corresponding to sample ω^{s} through formula (7), respectively.

(iii) Repeat the steps i and ii for r samples ω^{s} $(s=1,2,\ldots,r)$. The expected homogenized parameters $\widehat{S}$, $\widehat{k}_{ij}$, $\widehat{\beta}_{ij}$, $\widehat{\rho}$, and $\widehat{C}_{ijkl}$ are evaluated by formula (8).

(iv) With the expected homogenized parameters obtained by step iii, solve the homogenization problem (9) by using the finite-element difference method to obtain the homogenization solutions $T_0(x,t)$ and $\boldsymbol{u}_0(x,t)$.

(v) For the same sample ω^{s}, evaluate $M_{\alpha_1\alpha_2}(y,\omega^{\mathrm{s}})$, $R_{\alpha_1\alpha_2}(y,\omega^{\mathrm{s}})$, $Q_2(y,\omega^{\mathrm{s}})$, $\boldsymbol{N}_{\alpha_1\alpha_2}(y,\omega^{\mathrm{s}})$, $\boldsymbol{F}_2(y,\omega)$, and $\boldsymbol{P}_{\alpha_1}(y,\omega)$ by solving the problems (10)–(15), and using the same FE meshes as those in step ii.

(vi) Evaluate the derivatives of the homogenized solutions $T_0(x,t)$ and $\boldsymbol{u}_0(x,t)$ with respect to spatial variables by the average technique on relative elements[36] and the derivatives of those with respect to temporal variable by using the difference schemes in step iv.

(vii) The temperature and displacement distributions corresponding to the sample ω^{s} are evaluated from formulas (2) and (3). Then the thermal flux densities, strain and stress tensor are calculated through Eqs. (11)–(13), respectively.

4. Results and discussion

In this section, the dynamic thermo-mechanical response for a random particulate composite plate subjected to thermal shock is studied. We analyze the thermo-mechanical coupling effect and investigate the influences of the micro-characteristics of particles, including their shape, size, spatial

distribution, and volume fraction, on the macroscopic behaviors and thermo-mechanical coupling effect by using the software of SSOTS algorithm for the dynamic thermo-mechanical coupled problem developed by the authors.

For convenience, five different cell models with random distribution of particles are denoted as, Model 1:10% of uniformly distributed spherical particles; Model 2:20% of uniformly distributed spherical particles; Model 3:10% of normally distributed spherical particles around the centric point of a cell; Model 4:10% of uniformly distributed ellipsoidal particles whose long axes is about three times the middle axes and short axes, and which are subjected to normal distribution along the x_3 axis; Model 5:10% of uniformly distributed spherical particles whose diameter is 1.5 times those in Model 1. Furthermore, the radii are taken as 0.03 for the spherical particles of Models 1–3. The size of the ellipsoids' long axes in Model 4 is 0.09.

In Fig. 2, a composite plate made of ZrO_2 matrix reinforced by randomly distributed Ti-6Al-4V particles is shown. The entire plate has a height of 3.0, width of 8.0, and length of 10.0. In the following numerical computation, the material properties for the constituent materials are given in Table 1. The plate is clamped on its two-side surfaces in the x_2 direction. The temperature at the bottom and top surfaces are kept constant at 300 K and 1000 K, respectively. The initial temperature of the plate is 300 K.

Table 1. Material properties of Ti-6Al-4V and ZrO_2.

Property	Ti-6Al-4V	ZrO_2
Young modulus (E)/GPa	66.2	117.0
Poisson (ν)	0.321	0.333
Thermal modulus (β)/Pa·K^{-1}	1.90464×10^6	2.49063×10^6
Thermal conductivity (k)/W·mK^{-1}	18.1	2.036
Specific heat (c)/J·kgK^{-1}	808.3	615.6
Density (ρ)/kg·m^{-3}	4.41×10^3	5.6×10^3

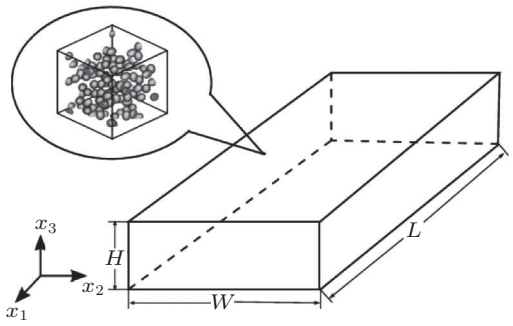


Fig. 2. Geometrical shape and coordinate system of the composite plate.

4.1. Macroscopic behaviors

Figure 3 shows the variation of the homogenized temperature and transverse displacement in the height direction at varying times until the composite plate reaches a steady state. The time variation of the homogenized temperature and transverse displacement at the point (4.0, 8.0, 2.8) for different volume fractions of Ti-6Al-4V particles is shown in Fig. 4. It is observed that the temperature increases more gradually with the increase in the volume fraction of particles. This is due to the fact that more Ti-6Al-4V particles means bigger effective thermal conductivity. The transverse displacement at the point increases rapidly to its maximum value at the beginning of thermal shocking and decreases to its steady state value. Moreover, the maximum value increases as the volume fraction of particles increases. Figure 5 illustrates the variation of the homogenized temperature and transverse displacement in the height direction for the plate composed of Models 1 and 3. It is clear that the temperature distribution with Model 3 is lower than that with Model 1. The reason is that most of particles in Model 3 are located around the center of the cell and the thermal conductivity of matrix is very low, which lead to the formation of thermal insulation. The distribution of transverse displacement with Model 1 is found to be lower than that with Model 3.

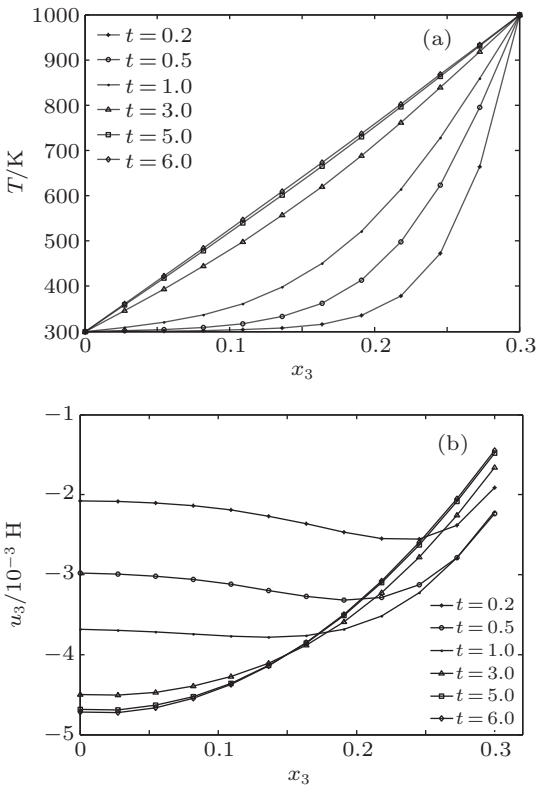


Fig. 3. Variation of (a) the homogenized temperature and (b) transverse displacement in the height direction.

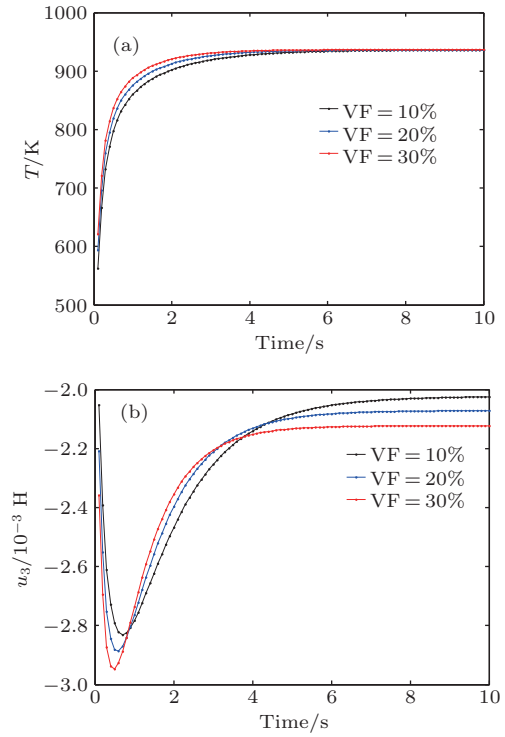


Fig. 4. (color online) Variation of (a) the homogenized temperature and (b) transverse displacement at the point (4.0, 8.0, 2.8) for different volume fractions of Ti-6Al-4V particles.

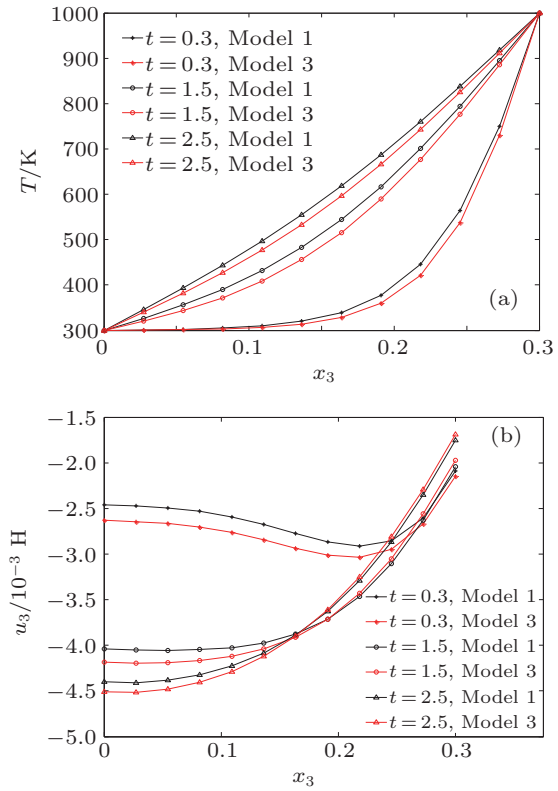


Fig. 5. (color online) Variation of (a) the homogenized temperature and (b) transverse displacement in the height direction for different cell models.

4.2. Thermo-mechanical coupling effect

Figure 6 shows the homogenized temperature and transverse displacement variations of coupled and uncoupled cases at the point (4.0, 8.0, 2.8). The variations of the coupled and uncoupled homogenized temperature and transverse displacement across the height direction are shown in Fig. 7. Figure 8 depicts the slices of the coupled and uncoupled homogenized temperature at time $t = 0.8$. The distributions of coupled and uncoupled SSOTS thermal flux densities and stresses in the cell located near the bottom of the plate at time $t = 0.8$ and $t = 10.0$ are presented in Figs. 9 and 10, respectively. It is observed from Figs. 6–10 that the difference between the coupled and uncoupled solutions is distinct and the coupling effect is missing with the lapse of time. It is also seen that the coupling effect decreases the temperature (Figs. 6(a), 7(a), and 8) and delays the propagation of thermal flux (Figs. 9(a), 9(b), 10(a), and 10(b)). The physical meaning of this phenomenon is that the coupling effect acts like a damper inside the composites, reduces the rate of heat propagation, and thus slows down the temperature rise. Figure 6(b) demonstrates that the coupling effect decreases the transverse displacement before it reaches the maximum value and then increases the transverse displacement after reaching the maximum value. In a word, the coupling effect causes a lag in the variations of temperature, thermal flux, displacement, and stresses. Moreover, we can obtain from Figs. 8–10 that the coupling effect in microscopic scale is relatively more distinct than that in macroscopic scale.

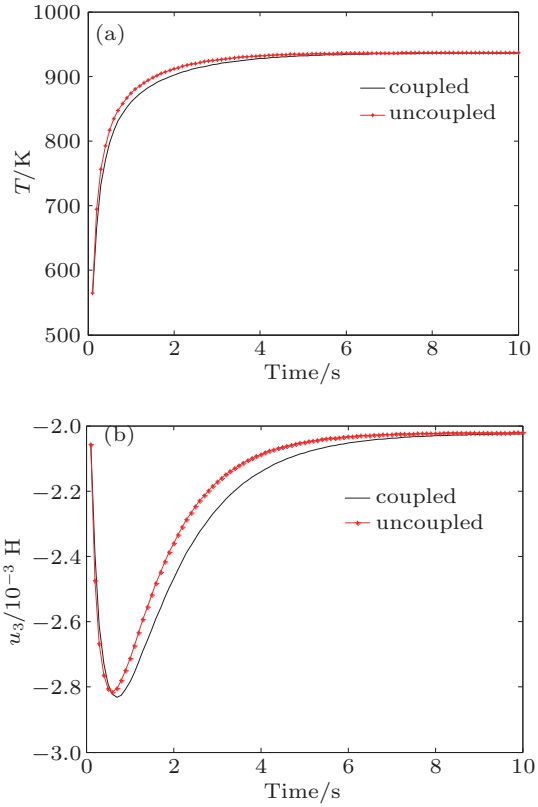


Fig. 6. (color online) Variation of the coupled and uncoupled solutions of (a) homogenized temperature and (b) transverse displacement at the point (4.0, 8.0, 2.8).

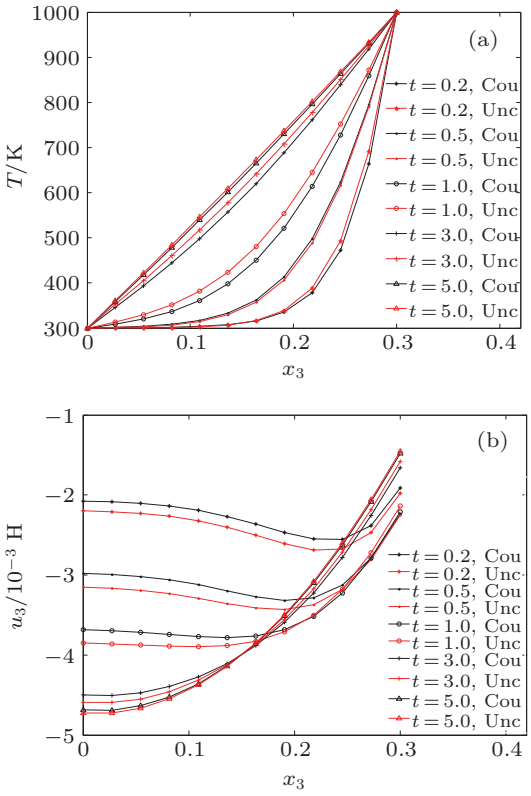


Fig. 7. (color online) Variation of the coupled (Cou) and uncoupled (Unc) solutions of (a) homogenized temperature and (b) transverse displacement in the height direction.

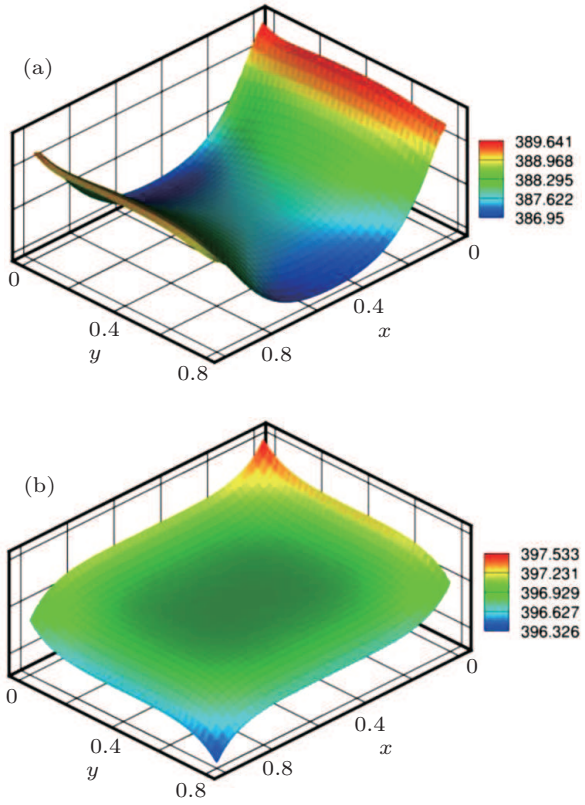


Fig. 8. (color online) Distributions of (a) coupled and (b) uncoupled homogenized temperature at time $t = 0.8$.

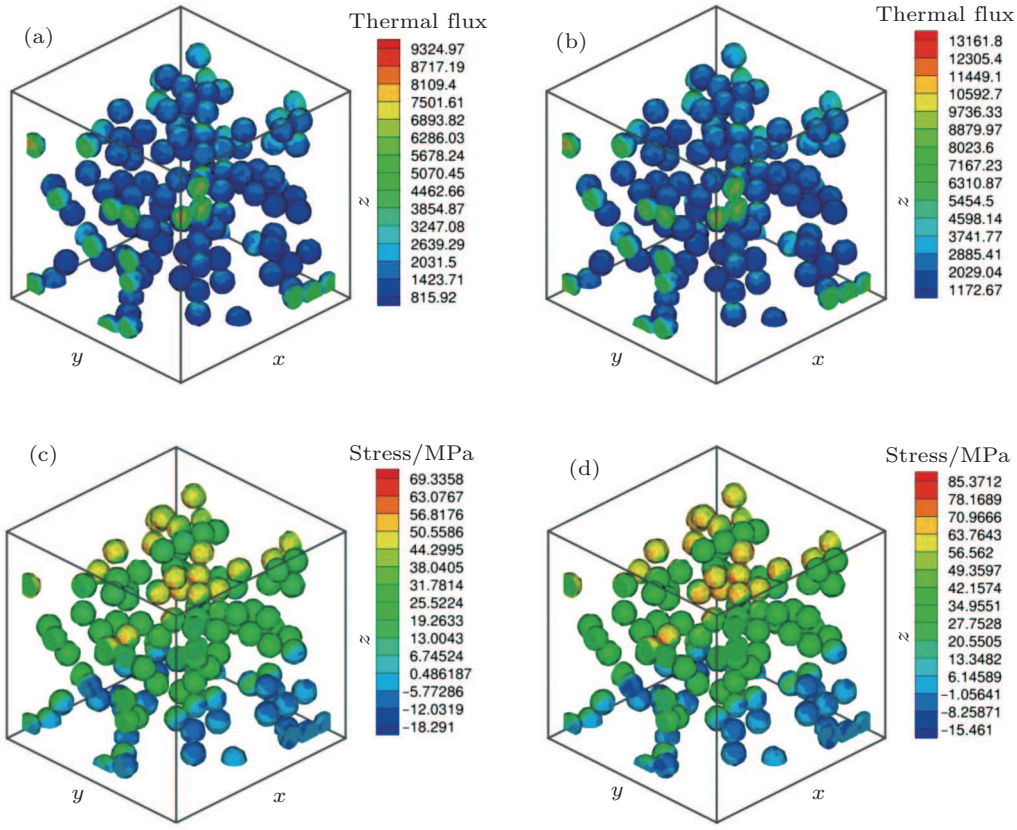


Fig. 9. (color online) Distributions of (a) coupled and (b) uncoupled thermal flux density and (c) coupled and (d) uncoupled stresses in the cell located near the bottom of the plate at time $t = 0.8$.

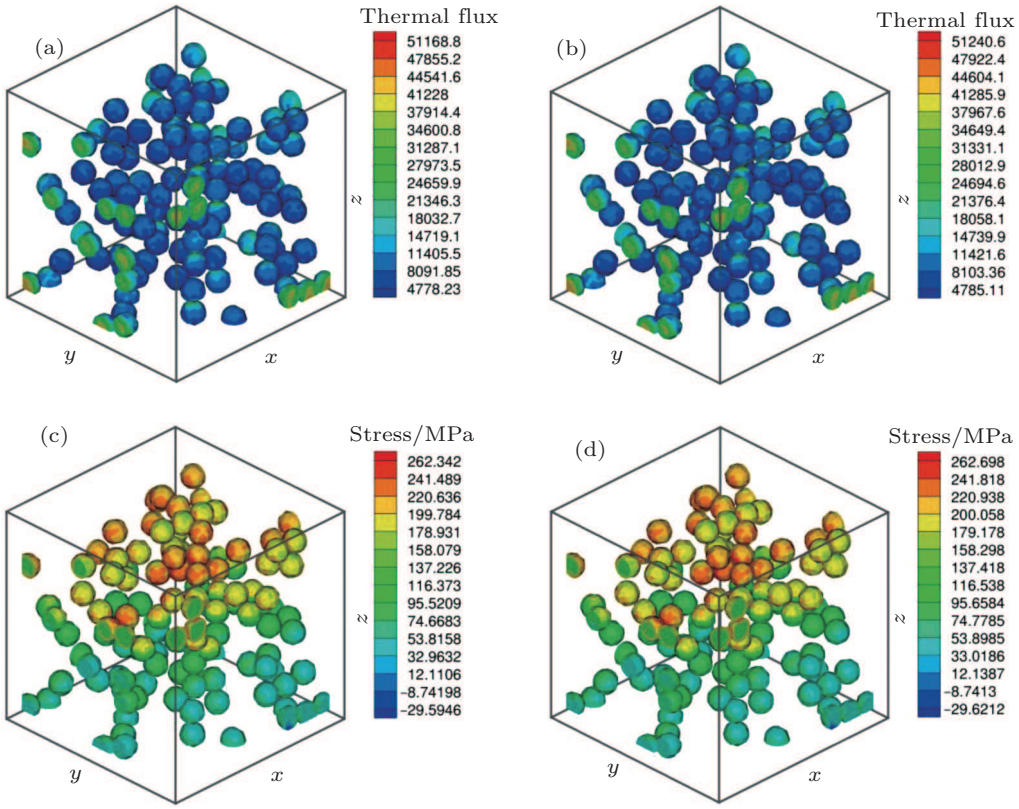


Fig. 10. (color online) Distributions of (a) coupled and (b) uncoupled thermal flux density and (c) coupled and (d) uncoupled stresses in the cell located near the bottom of the plate at time $t = 10.0$.

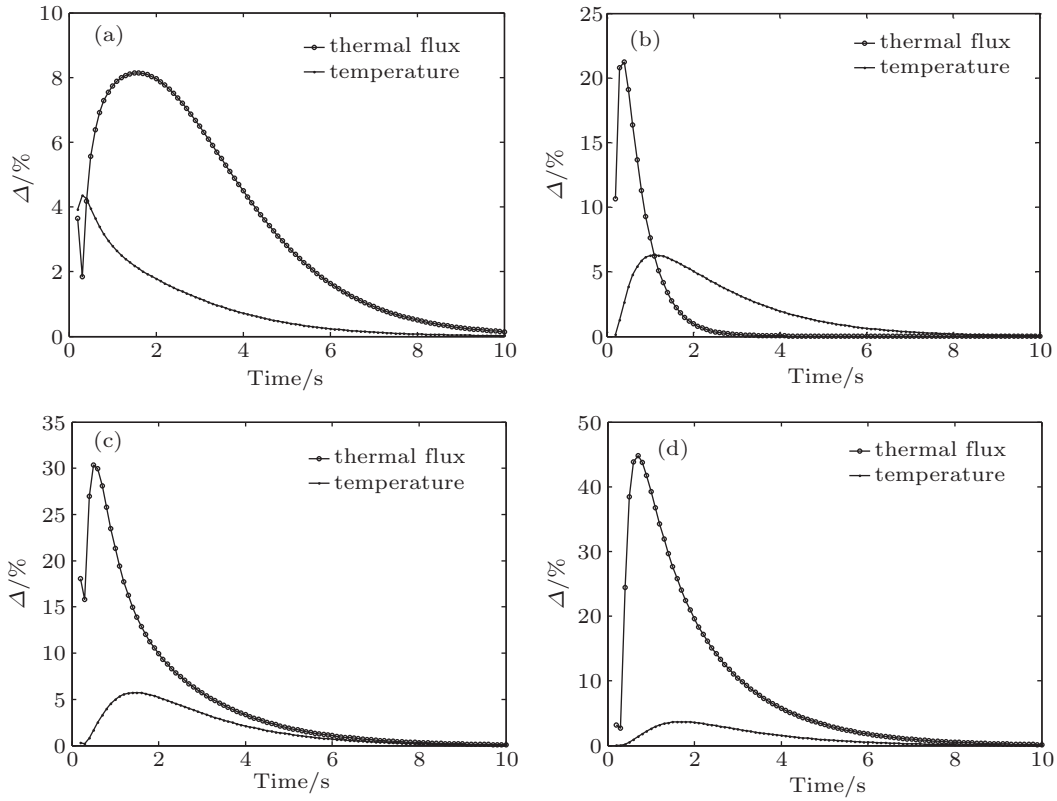


Fig. 11. The coupling effect of temperature and thermal flux density at the point (a) (4.0, 8.0, 2.5), (b) (4.0, 8.0, 1.5), (c) (4.0, 8.0, 1.0), and (d) (4.0, 8.0, 0.5).

In order to measure the distinction of the coupling effect, we define the notation Δ as follows:

$$\Delta = \left| \frac{\mathcal{D}_{\text{uncoupled}} - \mathcal{D}_{\text{coupled}}}{\mathcal{D}_{\text{coupled}}} \right|,$$

where $\mathcal{D}$ denotes the homogenized temperature, homogenized transverse displacement, or SSOTS solutions. Figure 11 shows the variations of the values of Δ for the SSOTS solutions of temperature and thermal flux density at the points (4.0, 8.0, 2.5), (4.0, 8.0, 1.5), (4.0, 8.0, 1.0), and (4.0, 8.0, 0.5), respectively. Figure 12 shows the distributions of values of Δ for those SSOTS solutions in the cell located near the top of the plate at time $t = 0.8$. It is easy to see that the coupling effect on the thermal flux density is much more distinct than that on the temperature. Moreover, figure 11 demonstrates that the influence of the coupling effect increases to its maximum value and then decreases gradually until it is missing. Figures 13 and 14 depcit the influences of cell models, including Models 1–4, on the values of Δ for homogenized temperature and transverse displacement at different locations. The results indicate that the influence of the micro-structures on the coupling effect is distinct.

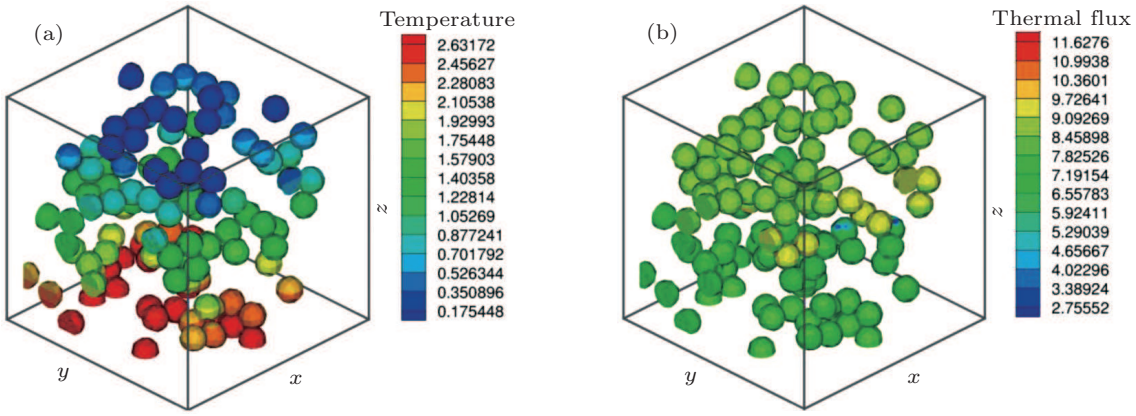


Fig. 12. (color online) Coupling effect of (a) the temperature and (b) thermal flux density in the cell located near the top of the plate at time $t = 0.8$.

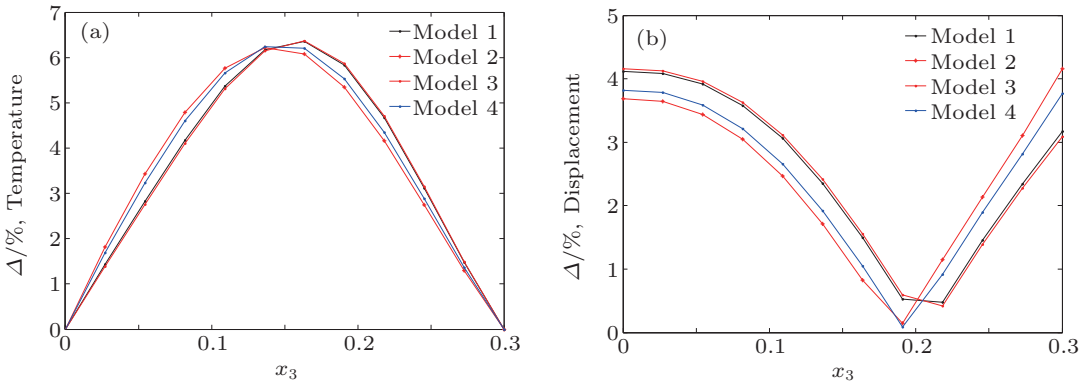
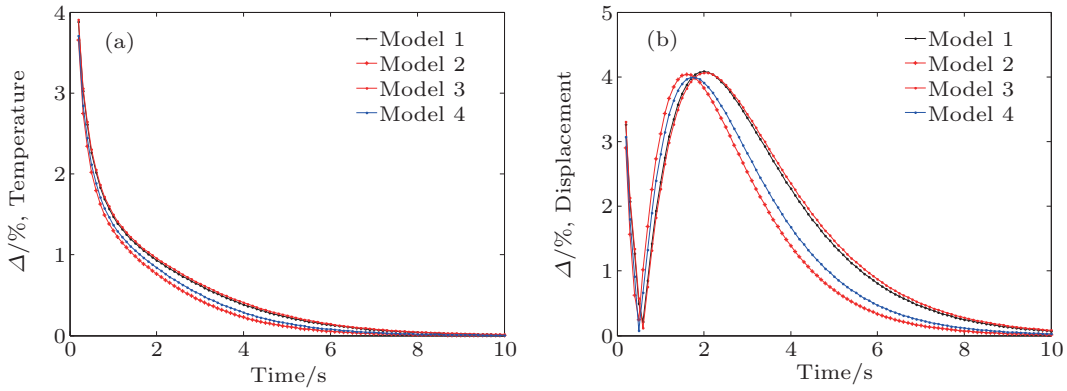


Fig. 13. (color online) Coupling effect of (a) the homogenized temperature and (b) transverse displacement in the height direction for different cell models at time $t = 0.8$.



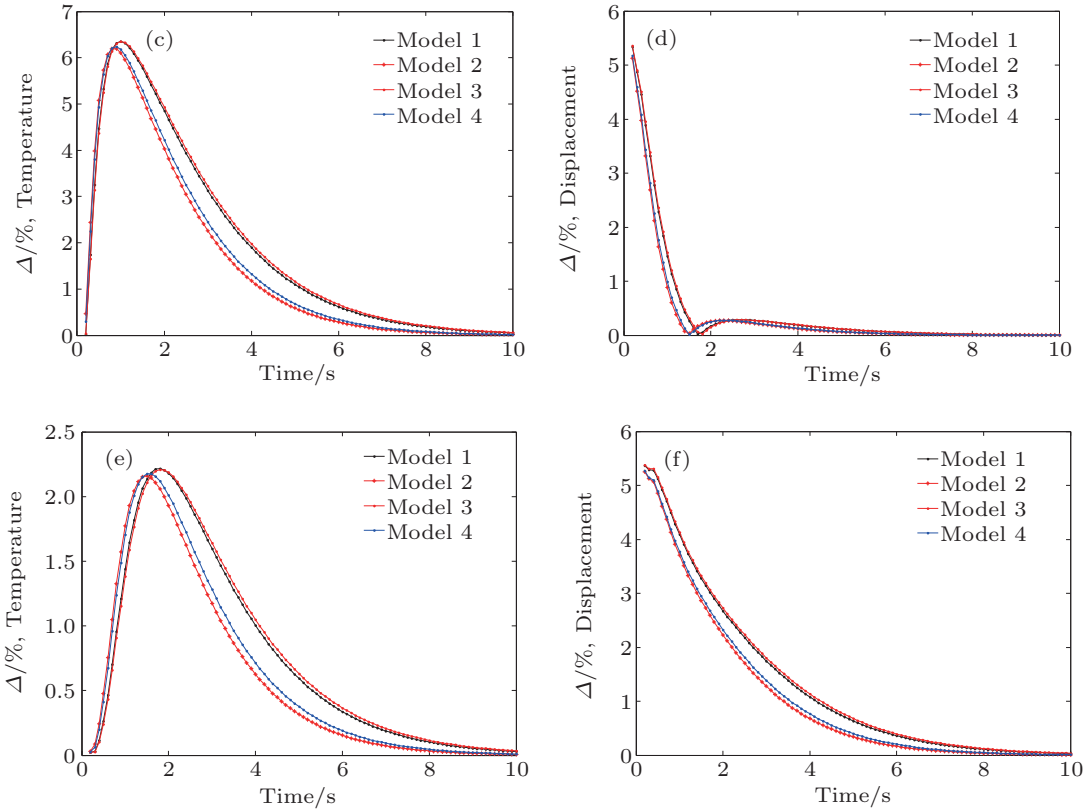


Fig. 14. (color online) Coupling effect of homogenized temperature and transverse displacement at the point (4.0, 8.0, 2.8) (a), (b), (4.0, 8.0, 1.6) (c), (d), and (4.0, 8.0, 0.28) (e), (f) for different cell models.

5. Conclusions

In this paper, we studied the dynamic thermo-mechanical coupled response of random particulate composites subjected to thermal shock. The coupled and uncoupled solutions of the temperature, thermal flux, displacement and stresses are obtained by using the SSOTS analysis method. We find that the coupling effects on the temperature, thermal flux, displacement, and stress are very distinct, which means that the coupling effect is significant in the dynamic thermo-mechanical response of random composites. Furthermore, the coupling effect in microscopic scale is found to be relatively more distinct than that in macroscopic scale and the coupling effect on the thermal flux is relatively much more distinct than that on the temperature in microscopic scale, which demonstrates that the micro-behaviors inside the composite material can be captured exactly by the SSOTS method. Besides, the results indicate that the coupling effect causes a lag in the variations of temperature, thermal flux, displacement, and stresses, and the micro-characteristics of particles have a great influence on the macroscopic behaviors and the coupling effect. As a result, the SSOTS analysis method can be used to investigate the dynamic thermo-mechanical coupled response, and is helpful to the design and optimization of random particulate composite materials.

References

[1] Biot M A 1956 *J. Appl. Phys.* **27** 240
[2] Boley B and Weiner J 1960 *Theory of Thermal Stress* (New York: John Wiley)
[3] Takeuti Y and Furukawa T 1981 *J. Appl. Mech.* **48** 113
[4] Abd-Alla A, Mahmoud S and Abo-Dahab S 2012 *Meccanica* **47** 1295
[5] Danilovskaya V 1950 *Prikl. Mat. Mekh.* **14** 316
[6] Yang Y C and Chu S S 2001 *Int. Commun. Heat. Mass.* **28** 1103
[7] Manoach E and Ribeiro P 2004 *Int. J. Mech. Sci.* **46** 1589
[8] Hetnarski R B and Eslami M R 2008 *Thermal Stresses: Advanced Theory and Applications* (Berlin: Springer Verlag)
[9] Kögl M and Gaul L 2003 *Arch. Appl. Mech.* **73** 377
[10] Ma Y E and Sun Q 2007 *J. Mech. Strength.* **29** 483
[11] Lee H L, Yang Y C and Chu S S 2002 *J. Therm. Stresses* **25** 1105
[12] Farhat C, Park K and Dubois-Pelerin Y 1991 *Comput. Meth. Appl. M.* **85** 349
[13] Feng Y P and Cui J Z 2003 *Acta Mech. Sin.* **19** 585
[14] Zhang H, Zhang S, Bi J and Schrefler B 2007 *Int. J. Numer. Meth. Eng.* **69** 87
[15] Yu W and Tang T 2007 *Int. J. Solids Struct.* **44** 3738
[16] Aboudi J, Pindera M and Arnold S 2001 *J. Appl. Mech.* **68** 697
[17] Terada K, Kurumatani M, Ushida T and Kikuchi N 2010 *Comput. Mech.* **46** 269
[18] Abbas I A, Kumar R and Chawla V 2012 *Chin. Phys. B* **21** 084601
[19] Francfort G A 1983 *SIAM J. Math. Anal.* **14** 696
[20] Parnell W J 2006 *J. Eng. Math.* **56** 1
[21] Aboudi J 2008 *J. Eng. Math.* **61** 111
[22] Khan K A, Barello R, Muliana A H and Lévesque M 2011 *Mech. Mater.* **43** 608
[23] Vel S S and Goupee A J 2010 *Comput. Mater. Sci.* **48** 22
[24] Cioranescu D and Donato P 2000 *An Introduction to Homogenization* (New York: Oxford University Press)
[25] Cui J Z, Shin T M and Wang Y L 1999 *Strcut. Eng. Mech.* **7** 601

[26] Yang Z Q, Cui J Z and Li B W 2014 *Chin. Phys. B* **23** 030203
[27] Feng Y P, Cui J Z and Deng M X 2009 *Acta Phys. Sin.* **58** 327 (in Chinese)
[28] Wan J J 2007 *Multi-Scale Analysis Method for Dynamic Coupled Thermoelasticity of Composite Structures* (Ph.D. Dissertation) (Beijing: Academy of Mathematics and System Sciences) (in Chinese)
[29] Li Y Y and Cui J Z 2004 *Sci. China Ser. A: Math.* **47** 101
[30] Li Y Y and Cui J Z 2005 *Compos. Sci. Technol.* **65** 1447
[31] Han F, Cui J Z and Yu Y 2009 *Acta Phys. Sin.* **58** S1 (in Chinese)
[32] Yang Z H and Cui J Z 2013 *Comput. Mater. Sci.* **69** 359
[33] Yu Y, Cui J Z and Han F 2008 *Compos. Sci. Technol.* **68** 2543
[34] Han F 2010 *The Second-Order Two-Scale Method for Predicting Mechanical Performance of Random Composite Materials* (Ph.D. Dissertation) (Xi'an: Northwestern Polytechnical University) (in Chinese)
[35] Reddy J N 1993 *An Introduction to the Finite Element Method* (New York: McGraw-Hill)
[36] Cui J Z 2001 *Invited Presentation on 'Chinese Conference of Computational Mechanics, CCCM*-2001*' in Proceedings on 'Computational Mechanics in Science and Engineering'*, December 5–8, 2001 Peking, China, p. 33